

Combination of Dual-Model-Base Adaptive Sampling Algorithm and Adaptive Cross Approximation for Fast Computation of Broadband RCS

Ziyue Cheng, Yueyuan Zhang*, Longfeng Xi, and Zhiwei Liu

Abstract—In this paper, a dual-model based adaptive sampling method is proposed for the fast calculation of broadband electromagnetic scattering. The difference between the rational function model (RFM) and cubic-spline (CS) based polynomial model is used to generate new frequency samples adaptively. Then, the cubic Hermite interpolation is used to approximate the final broadband RCS curve. The radar cross section (RCS) at each frequency sample is computed by the method of moment (MoM) which is accelerated by the adaptive cross approximation (ACA). Numerical results demonstrate that the proposed method is able to obtain the broadband RCS curve with high accuracy and reduce the computation time significantly. Compared with the method of moment and adaptive cross approximation method, the adaptive algorithm improves the computational efficiency by 77.13% in the sphere case, 83.79% in the rail model, and nearly 90.72% in the missile example. In addition, the method proposed in this paper has the characteristics of nonuniform sampling and strong applicability and flexibility, which is able to combine other matrix compressed methods to effectively solve problems in electromagnetic field.

1. INTRODUCTION

The analysis of broadband electromagnetic (EM) scattering problems is of great significance for obtaining the complete and effective features of the targets. It is mainly applied in stealth technology, geological exploration, EM compatibility problems, etc. The integral equation (IE) method is suitable for the calculation of broadband EM scattering problems due to its wide applicability and high accuracy [1].

The moment of method (MoM) is conventionally applied in the frequency domain integral equation (FDIE) method, which significantly reduces the complexity of computation and storage by transforming linear operators into algebraic equations [2, 3]. However, it still consumes massive time and storage to calculate frequency information and fill high-order dense matrix for the broadband target. The efficiency of MoM has been enhanced by the pointwise method, which includes fast Fourier transform [4], multilevel fast multipole algorithm (MLFMA) [5], and adaptive cross approximation (ACA) [6–8]. At present, some acceleration technologies related to MoM [9–11] have been able to solve large integral equations with millions of unknowns. Besides, some interpolation techniques, such as the model-based parameter estimation (MBPE) [12, 13], asymptotic waveform evaluation (AWE) [14, 15], Chebyshev approximation [16], and the reduced basis method (RBM) [17], are able to accurately compute the wideband response with a few direct calculations. In the AWE method, a large amount of high-order derivative information needs to be calculated and restored, and the accuracy of this method is limited by Taylor series. For Chebyshev approximation, it is preferred to the calculation of far-field than the

Received 12 November 2021, Accepted 21 December 2021, Scheduled 9 January 2022

* Corresponding author: Yueyuan Zhang (zyyaney1981@hotmail.com).

The authors are with the Department of Information Engineering, East China Jiaotong University, Nanchang, Jiangxi, China.

near-field. The RBM is a good interpolation method to solve the wideband EM problems while it is not feasible for electrically large targets without the combination of other algorithms [18]. Compared with aforementioned interpolation techniques, MBPE method does not need to calculate high-order derivative information and has the characteristics of strong applicability and flexibility. According to different objects, the interpolation algorithm can be applied to impedance matrix [19], induced current [20, 21], and RCS [22, 23], even scattering field.

The selection of samples is a common problem for all interpolation techniques, which determines the accuracy of approximate results and the total calculation time. Adaptive sampling algorithm has been proposed to solve the above difficulties [24–32]. The extended frequency points is usually selected to achieve the adaptive effect in AWE method [24–26]. A dichotomy method is proposed to select the expansion point through the midpoint in [24], and in [25] the single point and two-point AWE techniques are applied to the analysis of broadband EM problems. Multi-point AWE method is obtained by the combination of complex frequency hopping (CFH) technology in [26]. For other interpolation algorithms, the simplest way to select a sampling point is through the relative error of two adjacent samples [27]. In [18], an interpolation error verification process is added to select the sampling points. At the same time, an adaptive segmentation strategy is proposed in [28], which selects the samples in each paragraph. In addition, minimal rational interpolation has been developed [29], and Chebyshev algorithm is combined with MBPE sometimes [30]. Control factor is crucial for adaptive sampling algorithm. It can be a single value or some kind of error, which affects the sampling process. However, in the above-mentioned interpolation techniques, the control factor is usually calculated by the samples obtained by a certain interpolation method or model. There may be inaccuracies in a single method or model. In this regard, some scholars put forward the double model method which combined the cubic-spline (CS) and polynomial model [31, 32]. Polynomial interpolation is prone to wild oscillations, and an acceptable accuracy is sometimes achieved only by polynomials of intolerably high degree [33]. In this paper, a dual-model based adaptive sampling method is proposed to achieve nonuniform sampling. The sampling points are determined by the combination of rational function model (RFM) and CS model. Furthermore, the ACA is combined to accelerate the overall computing time. Numerical experiments demonstrate the validity of the bandwidth interpolation approach for the dual-model adaptive method. It is worth mentioning that the dual-model strategy is mainly used to interpolate the radar cross section (RCS) of the wideband target in this paper. However, the proposed algorithm has the characteristics of flexibility and universality, which does not rely on the calculation method, but only interpolates the calculated results. It can be applied to various occasions such as induced current and impedance matrix in combination with different calculation methods.

The remainder of the article is organized as follows. MoM-SIE and ACA will be introduced in Section 2. The adaptive sampling strategy is described in Section 3. Numerical case and results are given in Section 4. Conclusions and discussions are provided in Section 5.

2. CFIE FORMULATIONS AND ACA

In the surface integral equation (SIE) based on MoM technique, the resonance problem can be avoided by using the combined field integral equation (CFIE). Rao-Wilton-Glisson (RWG) [34] basis functions is used for surface modeling in the broadband target, and after Galerkin's testing the resulting linear system of MoM is obtained. The basis function and test function are represented by Λ_n and Λ_m , respectively. For a perfect electrical conductor object, the resulting linear systems from the CFIE formulation are briefly outlined as follows:

$$\sum_{n=1}^N Z_{mn} I_n = V_m, \quad m = 1, 2, \dots, N \quad (1)$$

$$Z_{mn} = \frac{\alpha}{\eta} Z_{mn}^{EFIE} + (1 - \alpha) Z_{mn}^{MFIE}, \quad (2)$$

$$Z_{mn}^{EFIE} = jk\eta \int_{S_m} \Lambda_m \cdot \int_{S_n} \left(\bar{\bar{I}} + \frac{\nabla \nabla}{k^2} \right) G(r, r') \cdot \Lambda_n ds' ds, \quad (3)$$

$$Z_{mn}^{MFIE} = \frac{1}{2} \int_{S_m} \Lambda_m \Lambda_n dr - \int_{S_m} \Lambda_m \cdot \hat{n} \times \int_{S_m} \nabla G(r, r') \times \Lambda_n ds' ds, \quad (4)$$

$$V_m = \int_{S_m} \Lambda_m \cdot \left[\alpha \frac{E^{inc}}{\eta} + (1 - \alpha) \hat{n} \times H^{inc} \right] ds. \quad (5)$$

here $G(r, r')$ represents the Green's function. η and k denote the wave number and wave impedance in free space, respectively. $\mathbf{E}^{inc}(\mathbf{r})$ and $\mathbf{H}^{inc}(\mathbf{r})$ is the incident excitation plane wave. \hat{n} is the external unit normal vector of PEC. I_n is the unknown expansion coefficient of the discrete current vector. For the dielectric target, it has different boundary constraints, and Poggio-Miller-Chang-Harrington-Wu-Tsai (PMCHWT) equation is used. The impedance matrix and excitation vector are given in Eqs. (6)–(11)

$$Z_{mm}^{EJ} = jk\eta \int_{S_m} \Lambda_m \cdot \int_{S_n} \bar{G}(r, r') \cdot \Lambda_n ds' ds - jk_d \eta_d \int_{S_m} \Lambda_m \cdot \int_{S_n} \bar{G}_d(r, r') \cdot \Lambda_n ds' ds, \quad (6)$$

$$Z_{mm}^{EM} = \int_{S_m} \Lambda_m \cdot \int_{S_n} \nabla G(r, r') \times \Lambda_n ds' ds - \int_{S_m} \Lambda_m \cdot \int_{S_n} \nabla G_d(r, r') \times \Lambda_n ds' ds, \quad (7)$$

$$Z_{mm}^{HJ} = - \int_{S_m} \Lambda_m \cdot \int_{S_n} \nabla G(r, r') \times \Lambda_n ds' ds + \int_{S_m} \Lambda_m \cdot \int_{S_n} \nabla G_d(r, r') \times \Lambda_n ds' ds, \quad (8)$$

$$Z_{mm}^{HM} = j \frac{k}{\eta} \int_{S_m} \Lambda_m \cdot \int_{S_n} \bar{G}(r, r') \cdot \Lambda_n ds' ds - j \frac{k_d}{\eta_d} \int_{S_m} \Lambda_m \cdot \int_{S_n} \bar{G}_d(r, r') \cdot \Lambda_n ds' ds, \quad (9)$$

$$V_m^E = \int_{S_m} \Lambda_m \cdot E^{inc} ds, \quad (10)$$

$$V_m^H = \int_{S_m} \Lambda_m \cdot H^{inc} ds. \quad (11)$$

To make further efforts in accelerating the efficiency of MoM, ACA algorithm is used to compress and simplify the impedance matrix. The ACA algorithm is mainly applied in the low-rank matrix compression, and it approximates a rank deficient matrix by a product of two matrices in an iterative manner. For the impedance matrix, it can be applied as:

$$\tilde{Z}^{m \times n} = U^{m \times r} \cdot V^{r \times n}. \quad (12)$$

A complete listing of the ACA algorithm is given in [6, 7]. ACA approximates an $m \times n$ element matrix block in k steps. In every step, the algorithm fills a row and a column of the original matrix with the maximum amplitude of the previous calculated ones, and then evaluates the approximation error. The goal of the ACA is to achieve Eq. (13),

$$\| \tilde{R}^{m \times n} \| = \| Z^{m \times n} - \tilde{Z}^{m \times n} \| \leq \varepsilon \| Z^{m \times n} \|. \quad (13)$$

For a given tolerance ε , \tilde{R} is termed as the error matrix. In addition, the impedance matrix is divided into many matrix blocks by using the octree structure, and each matrix block is calculated separately by ACA. The position of the required multiplication is found through the index label information in the matrix vector multiplication calculation, which can realize the overall calculation of different blocks and effectively reduce the storage memory and time of calculation. Finally, CPU time and memory overhead can be reduced to $O(N \log N)$.

3. ADAPTIVE SAMPLING STRATEGY

In this paper, a new adaptive sampling method is proposed to quickly calculate the RCS of wideband object. The dual-model algorithm is mainly based on cubic spline model and ration function model.

3.1. Cubic-Spline Interpolation Method

Cubic spline model makes full use of derivative information, so that it has better interpolation effect, while it is a difficult part to calculate and obtain the derivative value. The CS model is obtained mainly through two parts: one is to establish the cubic Hermite interpolation model, and the other is to obtain the corresponding derivative information through the continuity characteristics of the spline function.

Assume that the sampling points are x_0, x_1, \dots, x_n , $y = f(x)$, and the Hermite polynomial can be expressed as:

$$I_{2n+1}(x) = y_0\alpha_0(x) + \dots + y_n\alpha_n(x) + y'_0\beta_0(x) + \dots + y'_n\beta_n(x), \quad (14)$$

where the corresponding functions $\alpha_i(x)$ and $\beta_i(x)$ satisfy the following conditions:

$$\begin{aligned} \alpha_i(x_j) &= \delta_{ij} = \begin{cases} 1 & i = j \\ 0 & i \neq j \end{cases} & \beta_i(x_j) &= 0, \\ \alpha'_i(x_j) &= 0 & \beta_i(x_j) &= \delta_{ij} = \begin{cases} 1 & i = j \\ 0 & i \neq j \end{cases}. \end{aligned} \quad (15)$$

Since higher-order polynomials lead to the probability of Runge phenomenon, cubic segmentation method is selected. There can be a third-order polynomial at every two points, whose formula can be expressed as

$$I_1(x) = y_{k-1}\alpha_{k-1}(x) + y_k\alpha_k(x) + y'_{k-1}\beta_{k-1}(x) + y'_k\beta_k(x), \quad (16)$$

where k represents any segment divided by sampling points. $I_1(x)$ can be expanded as a third-order polynomial on x , and the interpolation model obtained from condition (15) can be described as

$$\begin{aligned} I_1(x) &= \frac{(x-x_i)^2[h_i+2(x-x_{i-1})]}{h_i^3}I_1(x_{i-1}) + \frac{(x-x_{i-1})^2[h_i+2(x-x_{i-1})]}{h_i^3}I_1(x_i) \\ &+ \frac{(x-x_i)^2(x-x_{i-1})}{h_i^2}I'_1(x_{i-1}) + \frac{(x-x_{i-1})^2(x-x_i)}{h_i^2}I'_1(x_i). \end{aligned} \quad (17)$$

The interval between two adjacent samples is expressed as $h_i = x_i - x_{i-1}$. To estimate the value of $I_1(x)$ in the frequency range, derivative information is needed, which can be solved by the derivative continuity of the spline function. The specific calculation process has been discussed in [31].

3.2. Rational Function Interpolation Method

Compared with polynomial model, rational function model is more flexible and has better approximation effect, and the formula of rational function is defined as

$$I_2(x) = \frac{a_0 + a_1x + a_2x^2 + \dots + a_px^p}{1 + b_1x + b_2x^2 + \dots + b_qx^q}, \quad (18)$$

where a and b are the model coefficients in the numerator and denominator of RFM. There are $p+q+1$ model coefficients to be determined, and the polynomial degree of numerator and denominator should be as close as possible in the solving process of this paper, which satisfy the condition:

$$|p - q| \leq 1, \quad (19)$$

RFM strategy is a direct solution method of formula (18), and by transforming the formula, the corresponding coefficient matrix can be obtained. The values of a and b can be achieved by solving the matrix equation by Gaussian elimination method.

$$y_i(1 + b_1x_i + b_2x_i^2 + \dots + b_qx_i^q) = a_0 + a_1x_i + a_2x_i^2 + \dots + a_px_i^p, \quad (20)$$

$$a_0 + a_1x_i + a_2x_i^2 + \dots + a_px_i^p - b_1x_iy_i - b_2x_i^2y_i - \dots - b_qx_i^qy_i = y_i, \quad (21)$$

$$\begin{bmatrix} 1 & x_0 & \dots & x_0^p & -x_0y_0 & \dots & -x_0^qy_0 \\ \vdots & \vdots & \ddots & \vdots & \vdots & \ddots & \vdots \\ 1 & x_p & \dots & x_p^p & -x_py_p & \dots & -x_p^qy_p \\ 1 & x_{p+1} & \dots & x_{p+1}^p & -x_{p+1}y_{p+1} & \dots & -x_{p+1}^qy_{p+1} \\ \vdots & \vdots & \ddots & \vdots & \vdots & \ddots & \vdots \\ 1 & x_n & \dots & x_n^p & -x_ny_n & \dots & -x_n^qy_n \end{bmatrix} \begin{bmatrix} a_0 \\ \vdots \\ a_p \\ b_1 \\ \vdots \\ b_q \end{bmatrix} = \begin{bmatrix} y_0 \\ \vdots \\ y_n \end{bmatrix}. \quad (22)$$

The solution of RFM with Gaussian elimination method is simple and convenient to implement, but it may produce ill conditioned matrix and affect the solution accuracy as the matrix demotion rises.

3.3. Adaptive Dual-Model Sampling Strategy

CS model has better interpolation performance in part range, but its application scope is not as wide as RFM. The dual-model adaptive approach is proposed, with which the accuracy of the interpolation method can be effectively improved by adding new samples at the maximum difference between the results of the two models. The process of adaptive sampling algorithm is shown in Figure 1.

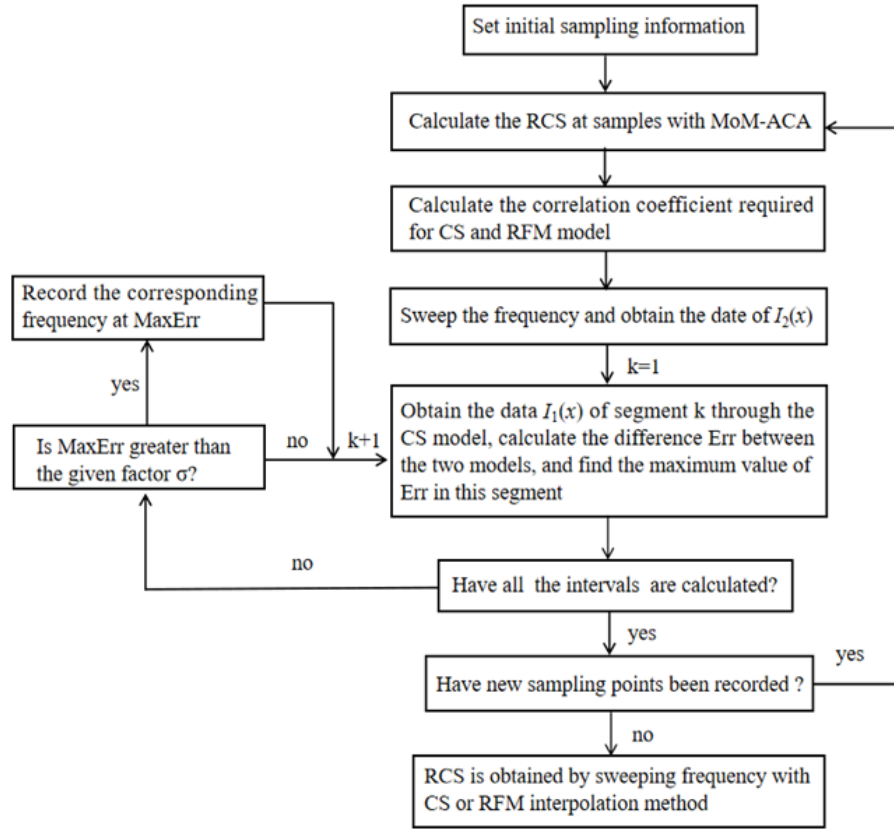


Figure 1. Flow chart of dual-model adaptive sampling algorithm.

There are several points needing attention in this method.

1. x and y in the model above correspond to the frequency and RCS of the target, respectively. Except for the samples calculated by MoM-ACA, the RCS data at other frequency points are evaluated by the proposed dual-model adaptive sampling method.
2. Due to the piecewise characteristics of spline function, the correlation coefficients of the two models are chosen to be calculated first, and the results of the two models are compared in each segment.
3. The value of control factor σ represents the difference between the two models. The adaptive strategy is mainly used with which the most informative samples are determined by different models so that the samples may not be accurate and need record when the calculation results of the two methods are quite different.
4. The condition for the end of the adaptive algorithm is that there are no new recording points in any section after a frequency sweep. Otherwise, the RCS at recorded frequency needs to be calculated by MoM-ACA method to cycle as a new sample. The specific algorithm steps of adaptive sampling method based on the above models are given as follows:

The frequency band and initial sampling points are known. N_{fs} denote the number of samples, and N_{fre} is the total number of sweep points. N_{fsnew} is used to represent the number of new samples added in an iteration. The error factor σ needs to set to control the algorithm process. A necessary

Algorithm 1 Dual-model adaptive sampling method.

Input: $f_{\min}, f_{\max}, \sigma, N_{fs}, N_{fre}$
Output: I, f_s, N_{fs}

- 1: Obtain the information of N_{fs} samples by dividing the frequency band equally;
 - 2: Calculate I at sampling point f_s by MoM-ACA;
 - 3: Calculate the coefficients in Eqs. (8) and (9). I', a, b , etc.;
 - 4: Sweep the frequency for number of N_{fre} points, $N_{fsnew} = 0$;
 For $N_{fs} - 1$ intervals, calculate I_1 and I_2 with two models, $\text{Err} = ||I_1 - I_2||$. Find the maximum value $\text{Err}[k]$ in each interval, if $\text{Err}[k] > \sigma$, record the corresponding frequency $f_t[k]$ and its number N_{fsnew} ;
 - 5: Until all intervals are calculated, if $N_{fsnew} > 0$, go to step 6, else go to step 7;
 - 6: Calculate I at the new samples by MoM-ACA, $N_{fs} = N_{fs} + N_{fsnew}$, divide the intervals according to f_s and update samples collection, skip back to step 3;
 - 7: CS method is used to sweep the frequency band, the algorithm ends.
-

step is to ensure the value of σ , and an appropriate value makes the proposed method more accurate and efficient. The method proposed in this paper can realize nonuniform sampling and does not depend on the algorithm process. It can be combined with any method to solve electromagnetic problems in frequency domain and time domain.

4. NUMERICAL RESULTS

To demonstrate the accuracy and efficiency of the proposed dual-model adaptive algorithm, the monostatic RCS examples from PEC sphere and rail dielectric missile are investigated. All experiments are conducted on a server with two 2.20 GHz Intel Xeon Silver 4114 CPU and 128 GB RAM. The targets are illuminated by a plane wave, and the CFIE related parameter used for solution is 0.5. In addition, Feko in this paper is mainly used for algorithm accuracy verification. The main solution is MLFMA, and other configurations are default.

The metal sphere with 10616 unknowns works at the frequency range 500 MHz–700 MHz, and the radius of the sphere is 0.5 m. It is used to simply demonstrate the effectiveness of the proposed method. The rail model with 15165 unknowns is shown in Figure 2. The total length of the rail is 6 m; the width of the rail bottom is 1.5 m; and that of the rail head is about 0.7 m, 1.76 m from the top to bottom. The frequency range for metal rail and dielectric missile model both from 600 MHz to 800 MHz. The unknown number of the missile model is 13548, and the missile is 2.5 m from nose to tail, as shown in the figure below. Its relative permittivity is 2.0, and the incident angle and pitch angle for the three examples are set to 0° . In addition, two evaluation indexes of relative error and root mean square error (RMSE) are used in this paper.

$$RE = \left| \frac{I - I'}{I} \right|, \quad (23)$$

$$RMSE = \sqrt{\frac{\sum_{i=1}^n (I_i - I'_i)^2}{N_{fre}}}, \quad (24)$$

The relative error which has been given in Eq. (23) can directly reflect the accuracy of the calculation method, and RMSE described in Eq. (24) usually indicates the degree that the calculation result deviates from the true value. The smaller value the RMSE is, the higher the calculation accuracy is. In this paper, I represents the result calculated by MoM-ACA; I' is the result obtained by interpolation method; and N_{fre} is the total number of calculation points.

The simulation results of the sphere are shown in Figure 3. The initial sampling points of CS and rational interpolation methods are set to 25. In the adaptive algorithm in (a), the value of the factor

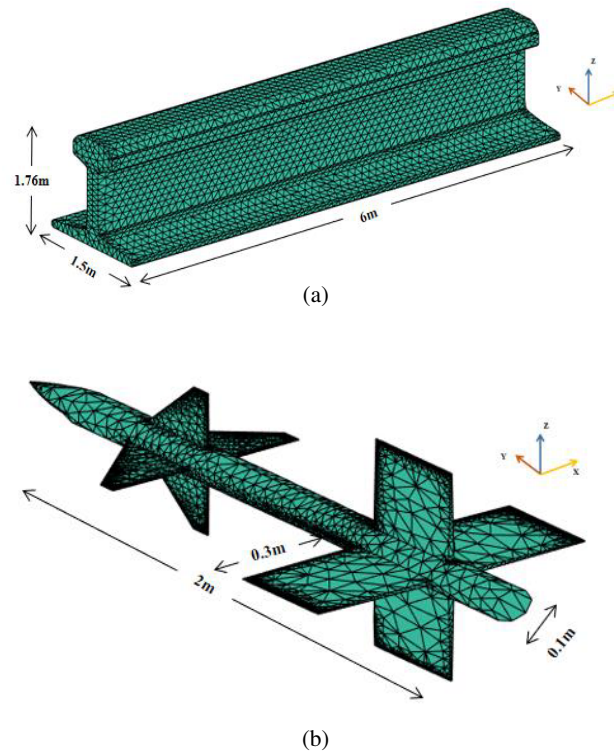


Figure 2. Simulation model: (a) rail; (b) missile.

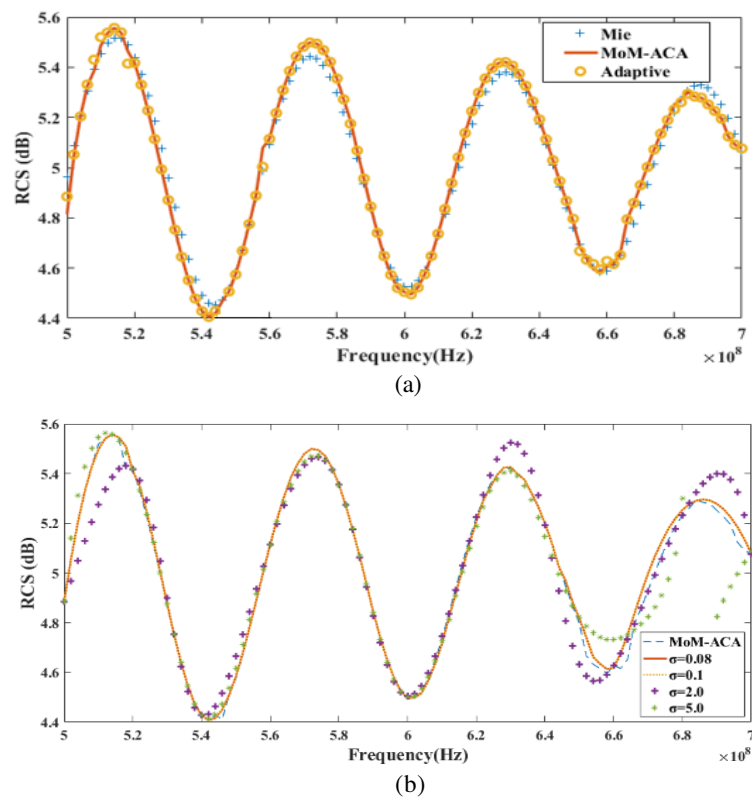


Figure 3. (a) RCS results of sphere; (b) The result of different values of termination factor.

σ is set to 0.1, and it can be seen that it fully approaches the reference result. The initial number of interpolation points is 10. Picture (b) shows the influence of termination factor on the calculation results in comparison. The smaller the value of σ is, the more accurate the calculation is, but the samples and calculation time will increase accordingly. The sampling points and time values of the sphere are given in Table 1.

Figure 4 shows the calculation results of the rail. The initial sampling points of CS and rational interpolation methods are set to 20. The number of initial samples in adaptive sampling method is 10, because too few points will lead to inaccurate calculation of the two models, which will affect the calculation accuracy. The final number of interpolation points is 18. Figure 4(b) shows the influence of different control factors σ on the interpolation results. In this example, the final value of σ is set

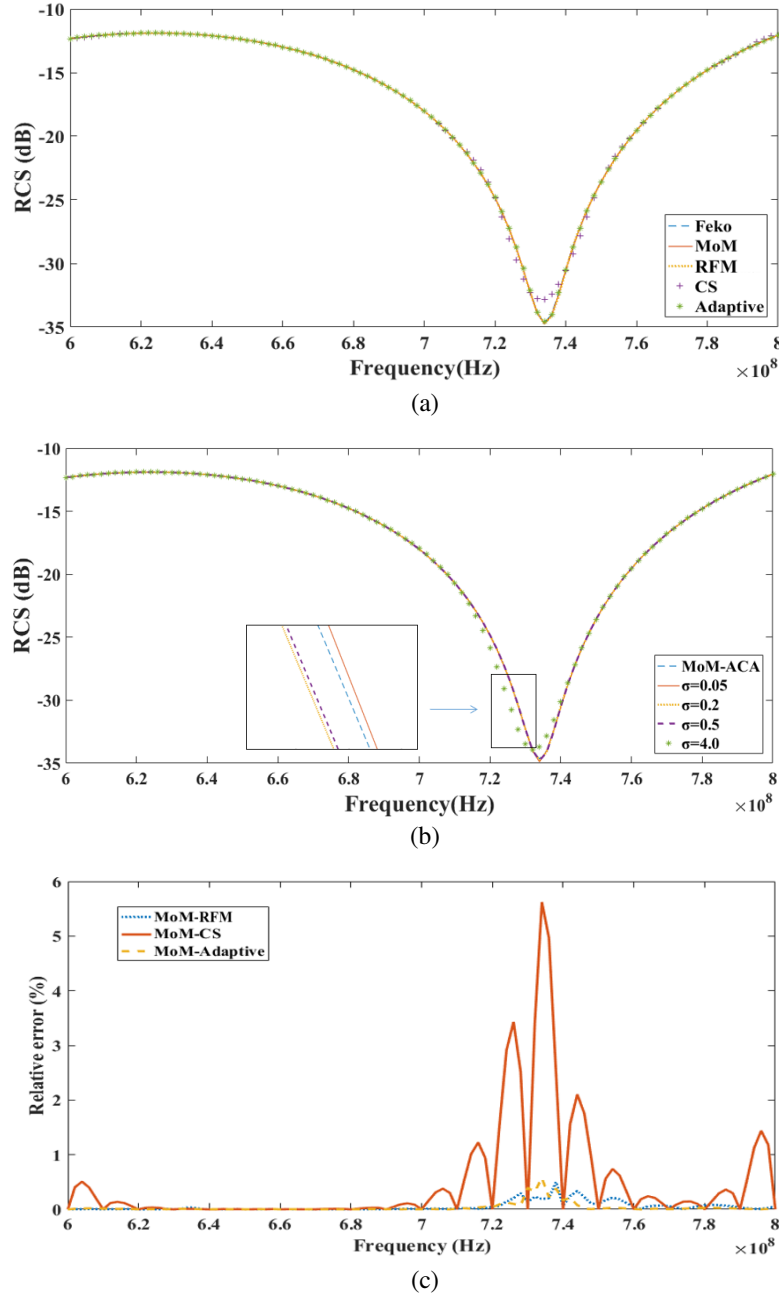


Figure 4. (a) RCS results of rail; (b) Relative errors of different interpolation algorithm.

Table 1. Calculation result of adaptive algorithm in sphere.

Method	MoM-ACA	Adaptive algorithm			
		$\sigma = 0.08$	$\sigma = 0.1$	$\sigma = 2.0$	$\sigma = 5.0$
Number of samples	100	49	24	19	16
Total time (hours)	3.76	1.42	0.86	0.62	0.53
RMES (dB)	/	0.260	0.261	0.0818	0.2291

Table 2. Calculation result of adaptive algorithm in rail.

Method	MoM-ACA	Adaptive ($\sigma = 0.5$)	CS	RFM
Number of samples	100	18	2	2
Total time (hours)	11.23	1.82	1.89	1.93
RMES (dB)	/	0.0287	0.3497	0.0316

Table 3. Calculation result of adaptive algorithm in missile.

Method	MoM-ACA	Adaptive ($\sigma = 1.0$)	CS	RFM
Number of samples	100	12	2	2
Total time (hours)	14.77	1.37	2.73	2.88
RMES (dB)	/	0.8466	0.8539	1.4010

0.5, because the number of samples is as high as 53 under the condition of 0.05, which seriously affects the efficiency of interpolation. In contrast, better fitting accuracy can be obtained under the condition of 0.5. It can be seen from Figure 4(c) and Table 2 that the adaptive selection of interpolation points through the comparison of the two models can effectively avoid the inaccurate calculation while an interpolation model is not very accurate. Inside, the reason for the large error of CS calculation may be the deviation caused by solving the derivative information.

The calculation results of dielectric missile are shown in Figure 5 below. In this part, the RFM and CS are not so accurate. It is speculated that it is due to the discontinuity of some points of the method of moment. Therefore, the initial number of sampling points in this example is set to 5. It can be seen that combining Figures 5(a) and (b), the adaptive interpolation proposed in this paper can select the sampling points with high information value and approach the curve more accurately with fewer samples. The data in Table 3 show that the adaptive algorithm is more efficient, and the result is more accurate than that of a single model.

Picture (c) shows the process of adaptive algorithm in this part actually. For the initial five sampling points, it is found that the calculation results of the two models are quite different between 700 MHz and 750 MHz after the first cycle. Therefore, the second cycle is carried out after adding one sampling point. After adding four samples in the second cycle, the process executes again, until the calculation difference between the two models at all frequencies is less than the given factor σ , and the sampling process is ended. The points of the corresponding color on each curve represent the newly added sampling points in this cycle. In this example, only 12 samples can achieve a better interpolation result.

The specific interpolation information is given in the table below. Compared with the method of moment and adaptive cross approximation method, the adaptive algorithm improves the computational efficiency by 77.13% in the sphere case, 83.79% in the rail model, and nearly 90.72% in the missile example. It can be seen in Table 3 that under certain circumstances, the computational efficiency of adaptive algorithm is nearly 50% higher than that of RFM and CS model, which is the most accurate interpolation method concluded from the RMSE results.

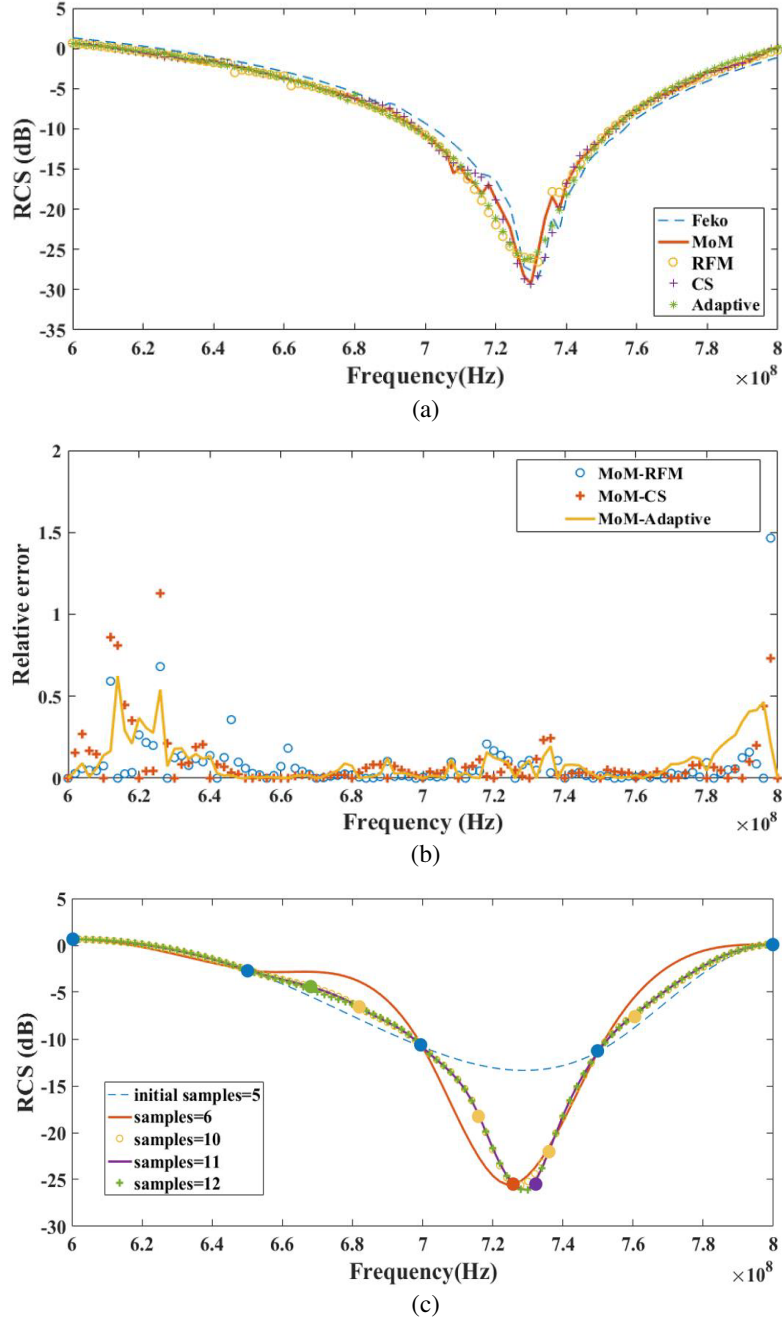


Figure 5. (a) RCS results of rail; (b) Relative errors of different interpolation algorithm.

5. CONCLUSION

A dual-model adaptive algorithm based on cubic-spline and rational function model is proposed for the calculation of RCS in broadband electromagnetic problems. This strategy is based on the platform of MoM, and ACA is used to accelerate the single point of computation. The characteristic of this method is nonuniform sampling and can avoid the inaccurate calculation of a single interpolation model. By properly selecting the judgment factor σ of the two model errors, the interpolation point position with the highest benefit can be selected independently. Examples of calculation are a metal sphere with an unknown quantity of 10616, a metal rail model with 15165 unknowns, and a dielectric missile with

an unknown quantity of 13548. Their computational efficiency is improved by 77.13%, 83.79%, and 90.72%, respectively. As a result, the proposed adaptive interpolation algorithm can approach the RCS curve precisely and efficiently. In fact, if the induced current is interpolated first, and then the RCS of the target is calculated, a better effect can be obtained, which is also the authors' next project. Besides, the adaptive sampling strategy does not depend on the process of other algorithms, but only for the characteristics of the results, so that it can be combined with any method to solve electromagnetic problems in frequency domain and time domain.

ACKNOWLEDGMENT

This work was supported by Jiangxi provincial Outstanding Youth Talent Project of Science and Technology Innovation (No. 20192BCBL23003), Natural Science Foundation of Jiangxi Province (No. 20202BAB202004) and National Nature Science Foundation of China for Youth under Grant 62001245.

REFERENCES

1. Lu, C. C. and W. C. Chew, "Fast algorithm for solving hybrid integral equations," *IEEE Proceedings — H*, Vol. 140, No. 6, 455–460, 1993.
2. Harrington, R. F., *Field Computation by Moment Methods*, Wiley-IEEE Press, 1993.
3. Gibson, W. C., *The Method of Moments in Electromagnetics*, Chapman & Hall/CRC, New York, 2008.
4. Seo, S. M., "A fast IE-FFT algorithm to analyze electrically large planar microstrip antenna arrays," *IEEE Antennas and Wireless Propagation Letters*, Vol. 17, No. 6, 983–987, Jun. 2018.
5. Liu, Y., X. Pan, and X. Sheng, "A fast algorithm for volume integral equation using interpolative decomposition and multilevel fast multipole algorithm," *2016 11th International Symposium on Antennas, Propagation and EM Theory (ISAPE)*, 519–522, 2016.
6. Bebendorf, M., "Approximation of boundary element matrices," *Numerische Mathematik*, Vol. 86, No. 4, 565–589, 2000.
7. Zhao, K. Z., M. N. Vouvakis, and J.-F. Lee, "The adaptive cross approximation algorithm for accelerated method of moments computations of EMC problems," *IEEE Transactions on Electromagnetic Compatibility*, Vol. 47, No. 4, 763–773, 2005.
8. Liu, Z., X. Wang, D. Tang, Y. Zhang, S. Jie, and X. Liu, "MLFMA-ACA based method for efficient calculation of scattering from underground targets," *2018 IEEE International Conference on Computational Electromagnetics (ICCEM)*, 1–3, 2018.
9. Carpentieri, B., I. S. Duff, L. Giraud, et al., "Combining fast multipole techniques and an approximate inverse preconditioner for large electromagnetism calculations," *SIAM Journal on Scientific Computing*, Vol. 27, No. 3, 774–792, 2005.
10. Pan, X., W. Pi, M. Yang, Z. Peng, and X. Sheng, "Solving problems with over one billion unknowns by the MLFMA," *IEEE Transactions on Antennas and Propagation*, Vol. 60, No. 5, 2571–2574, May 2012.
11. Carpentieri, B., "Algebraic preconditioners for the fast multipole method in electromagnetic scattering analysis from large structures: Trends and problems," *Electronic Journal of Boundary Elements*, Vol. 7, No. 1, 2009.
12. Miller, E. K., "Using adaptive sampling to minimize the number of samples needed to represent a transfer function," *IEEE Antennas and Propagation Society International Symposium. 1996 Digest*, Vol. 1, 588–591, Baltimore, MD, USA, 1996.
13. Miller, E. K., "Adaptive sparse sampling to estimate radiation and scattering patterns to a specified uncertainty with model-based parameter estimation: Compute patterns using as few as two to four samples per lobe," *IEEE Antennas and Propagation Magazine*, Vol. 57, No. 4, 103–113, Aug. 2015.
14. Cockrell, C. R. and F. B. Beck, "Asymptotic waveform evaluation (AWE) technique for frequency domain electromagnetic analysis," *NASA Tech. Memo.*, 110292, Nov. 1996.

15. Wu, B. and X. Sheng, "Application of asymptotic waveform evaluation to hybrid FE-BI-MLFMA for fast RCS computation over a frequency band," *IEEE Transactions on Antennas and Propagation*, Vol. 61, No. 5, 2597–2604, May 2013.
16. Jeong, Y., I. Hong, H. Chun, Y. B. Park, Y. Kim, and J. Yook, "Fast analysis over a wide band using Chebyshev approximation with Clenshaw-Lord approximation," *The 8th European Conference on Antennas and Propagation (EuCAP 2014)*, 1353–1355, 2014.
17. Monje-Real, A. and V. de la Rubia, "Electric field integral equation fast frequency sweep for scattering of nonpenetrable objects via the reduced-basis method," *IEEE Transactions on Antennas and Propagation*, Vol. 68, No. 8, 6232–6244, Aug. 2020.
18. Wu, L., et al., "MLACE-MLFMA combined with reduced basis method for efficient wideband electromagnetic scattering from metallic targets," *IEEE Transactions on Antennas and Propagation*, Vol. 67, No. 7, 4738–4747, Jul. 2019.
19. Kong, W., J. Xie, F. Zhou, X. Yang, R. Wang, and K. Zheng, "An efficient FG-FFT with optimal replacement scheme and inter/extrapolation method for analysis of electromagnetic scattering over a frequency band," *IEEE Access*, Vol. 7, 127511–127520, 2019.
20. Song, J. M. and W. C. Chew, "Broadband time-domain calculation using FISC," *IEEE Antennas and Propagation Society International Symposium*, 552, 2002.
21. Lu, C. C., "An extrapolation method based on current for rapid frequency and angle sweeps in far-field calculation in an integral equation algorithm," *ACES Journal*, Vol. 21, No. 1, 90–98, 2006.
22. Erdemli, Y. E., J. Gong, C. J. Reddy, and J. L. Volakis, "Fast RCS pattern fill using AWE technique," *IEEE Transactions on Antennas and Propagation*, Vol. 46, No. 11, 1752–1753, Nov. 1998.
23. Reddy, C. J., M. D. Deshpande, C. R. Cockrell, and F. B. Beck, "Fast RCS computation over a frequency band using method of moments in conjunction with asymptotic waveform evaluation technique," *IEEE Transactions on Antennas and Propagation*, Vol. 46, No. 8, 1229–1233, Aug. 1998.
24. Chew, W. C., J. M. Song, E. Michielssen, et al., *Fast and Efficient Algorithms in Computational Electromagnetics*, Artech House, Boston London, 2001.
25. Surma, M., "Efficient wideband analysis of electromagnetic scattering and radiation problems," *15th International Conference on Microwaves, Radar and Wireless Communications*, 291–294, 2004.
26. Peng, Z. and X. Sheng, "A bandwidth estimation approach for the asymptotic waveform evaluation technique," *IEEE Transactions on Antennas and Propagation*, Vol. 56, No. 3, 913–917, Mar. 2008.
27. Lehmensiek, R. and P. Meyer, "An efficient adaptive frequency sampling algorithm for model-based parameter estimation as applied to aggressive space mapping," *Microwave and Optical Technology Letters*, Vol. 24, No. 1, 71–78, 2000.
28. Wu, L., Y. Zhao, Q. Cai, Z. Zhang, and J. Hu, "An adaptive segmented reduced basis method for fast interpolating the wideband scattering of the dielectric-metallic targets," *IEEE Antennas and Wireless Propagation Letters*, Vol. 19, No. 12, 2235–2239, Dec. 2020.
29. Wu, J. W. and T. J. Cui, "Minimal rational interpolation and its application in fast broadband simulation," *IEEE Access*, Vol. 7, 177813–177826, 2019.
30. Wang, X., H. Gong, S. Zhang, Y. Liu, R. Yang, and C. Liu, "Efficient RCS computation over a broad frequency band using subdomain MoM and chebyshev approximation technique," *IEEE Access*, Vol. 8, 33522–33531, 2020.
31. Liu, Z. W., R. S. Chen, and J. Q. Chen, "Adaptive sampling cubic-spline interpolation method for efficient calculation of monostatic RCS," *Microwave and Optical Technology Letters*, Vol. 50, No. 3, 751–755, 2008.
32. Liu, Z. W., D. Z. Ding, Z. F. Fan, et al., "Adaptive sampling bicubic spline interpolation method for fast calculation of monostatic RCS," *Microwave and Optical Technology Letters*, Vol. 50, No. 7, 1851–1857, 2008.

33. Lehmensiek, R. and P. Meyer, "Creating accurate multivariate rational interpolation models of microwave circuits by using efficient adaptive sampling to minimize the number of computational electromagnetic analyses," *IEEE Transactions on Microwave Theory and Techniques*, Vol. 49, No. 8, 1419–1430, Aug. 2001.
34. Rao, S., D. Wilton, and A. Glisson, "Electromagnetic scattering by surfaces of arbitrary shape," *IEEE Transactions on Antennas and Propagation*, Vol. 30, No. 3, 409–418, May 1982.